Interaction of $C_{59}Si$ with Si based clusters: a study of Janus nanostructures

2010 J. Phys.: Condens. Matter 22 275303

(http://iopscience.iop.org/0953-8984/22/27/275303)

J. Phys.: Condens. Matter **22** (2010) 275303 (6pp) doi:10.1088/0953-8984/22/27/275303

Interaction of $C_{59}Si$ with Si based clusters: a study of Janus nanostructures

Miao Miao Wu[1,2], Xiao Zhou[1,2], Jian Zhou[1,2], Qiang Sun[1,2], Qian Wang[3] and Puru Jena[3]

[1] Department of Advanced Materials and Nanotechnology, Peking University, Beijing 100871, People's Republic of China
[2] Center for Applied Physics and Technology, Peking University, Beijing 100871, People's Republic of China
[3] Department of Physics, Virginia Commonwealth University, Richmond, VA 23284, USA

E-mail: sunqiang@pku.edu.cn

Received 8 February 2010, in final form 17 May 2010
Published 23 June 2010
Online at stacks.iop.org/JPhysCM/22/275303

Abstract

Using density functional theory with the generalized gradient approximation (GGA), we show that carbon–silicon Janus anisotropic nanostructures can be synthesized by using $C_{59}Si$ heterofullerene as a seed where the doped Si atom preferentially attaches to some well-known silicon and silicon based clusters such as Si_{10}, WSi_{12}, $TiSi_{16}$, and $BaSi_{20}$. The interaction energy of these clusters with $C_{59}Si$ varies from 0.9 to 1.9 eV. The anisotropy of the resulting carbon–silicon Janus structures produces large dipole moments (4–9 D), anisotropic distributions of electronic orbitals, and the anisotropic reactivity.

(Some figures in this article are in colour only in the electronic version)

1. Introduction

Nanoparticles, due to their small size and low dimensionality possess unique properties that differ from their bulk form. The large surface area of these particles and quantum confinement are mainly responsible for these properties. The minimization of surface energies usually leads nanoparticles to have spherical symmetry and hence these particles are not suitable as multifunctional materials. Consequently there has been a great deal of effort in recent years to synthesize anisotropic nanoparticles where different ends of the particle may have different properties. For example, one end may be hydrophilic while the other end is hydrophobic. These anisotropic nanoparticles have been termed by de Gennes [1] as Janus particles and the two hemispheres of these particles have different chemical character. However, synthesizing these Janus nanostructures has been a challenge. In this paper we study the interaction of Si-doped fullerene as a seed to promote anisotropic growth. We have concentrated on carbon–silicon Janus nanostructures for the following four reasons:

(1) Although both Si and C belong to the same group of elements in the periodic table, their chemistry is very different. For example, oxides of carbon, namely CO and CO_2, form gases, while oxides of silicon constitute common sand. Similarly the sp^2 and sp^3 bonding characteristics of carbon give rise to novel forms starting from the well-known planar graphite and tetrahedral diamond to 'spherical' fullerenes and cylindrical nanotubes. On the other hand, silicon prefers only tetrahedral bonding due to its larger core. Both carbon based nanostructures such as fullerenes and nanotubes [2, 3] as well as Si based nanostructures [4–8] have potential technological applications. This has led to recent interest in carbon–silicon composite nanostructures [6, 9, 10] which have great potential for applications in quantum dots, quantum wires, nonlinear electronic components and memory devices.

(2) Bulk silicon carbide is a well-known material with exceptional physical and mechanical properties, including low density, high strength, high thermal conductivity, stability at high temperature, high resistance to shock, low thermal expansion, high refractive index, wide (tunable) band gap and chemical inertness. We can expect that nanoscale carbon–silicon composite structures may exhibit novel properties due to the large surface area and quantum size effect. One of the well-known carbon–silicon nanostructures is $C_{60}@Si_{60}$, which was suggested by Harada and co-workers for stabilizing the Si_{60} cage with a C_{60} core. This complex has attracted extensive interest theoretically [11–16] and experimentally [17–24]. Unfortunately, the observation of $C_{60}@Si_{60}$ has remained

elusive [17–24]. In contrast, it has been found experimentally that Si_{60} is unlikely to wet the surface of C_{60} [22], and it has been theoretically confirmed that $C_{60}@Si_{60}$ is energetically unstable [7]. Due to the stability of the carbon fullerene cage, it is difficult to grow a silicon nanostructure directly on the C_{60} surface. In this study we show that fullerene substitutionally doped with Si provides us with an embryo for Si growth, with the Si site acting as the growth seed.

(3) Recently, a great deal of attention has been paid to the shape-controlled synthesis [25–30] of nanostructures with anisotropies that possess certain advantages over their spherical counterparts, as they can be dually functionalized for potential applications. Since C and Si have different properties, it is expected that carbon–silicon Janus nanostructures may have interesting properties.

(4) Silicon nanostructures such as Si_{10}, Si_{20}, $M@Si_n$ (M = Ti, W, Cr, Mo, Ba, n = 8–20) have been extensively studied both theoretically and experimentally, but one of the challenges for their application is how to assemble these structural units to make functional materials [8–10]. Here we show that Si-doped heterofullerene may provide a novel pathway for assembling carbon–silicon Janus nanostructures.

2. Computational methods

The calculations were carried out within the framework of density functional theory (DFT) and the generalized gradient approximation (GGA) for exchange–correlation energy for which the Perdew–Wang 91 (PW91) functional form [31] was used. In order to optimize the geometry effectively, a plane-wave basis set is adopted with the projector-augmented-wave (PAW) method, originally developed by Blochl [32] and recently adapted by Kresse and Joubert, as implemented in the *Vienna ab initio simulation package* (VASP) [33]. The particular advantage of the PAW method over the ultrasoft pseudopotentials is that the pseudization of the augmentation charge can be avoided. The structure optimization is symmetry unrestricted and carried out using the conjugate gradient algorithm. The convergence for energy and force were set to 0.0005 eV and 0.01 eV $Å^{-1}$, respectively. The kinetic energy cutoff used in our calculations is 300 eV. A supercell approach was used, where the clusters under investigation were surrounded by 15 Å of vacuum space along the x, y, and z directions, which is large enough to avoid the interactions with images. Due to the large supercell, the Γ point was used to represent the Brillouin zone. The accuracy of calculation for fullerene and Si based nanostructures has been extensively tested in our previous studies [6–8, 10]. For example, although GGA usually underestimates the HOMO–LUMO gap, our calculated value for C_{60} is 1.61 eV, which is comparable to the experimental value of 1.68 eV. GGA + U is better, especially for systems containing d- or f-electrons; for our studied systems $C_{59}Si$ + Si-clusters, the corrections of GGA + U would be small.

3. Results and discussion

We begin with the structure of $C_{59}Si$ where a C atom in the C_{60} fullerene has been substituted with a Si atom.

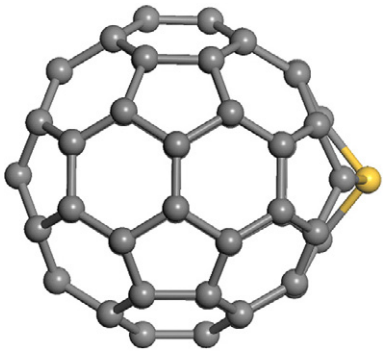

Figure 1. Geometry of $C_{59}Si$ cluster.

This heterofullerene was synthesized in 1996 using the laser vaporization cluster beam technique. Our optimization of the $C_{59}Si$ geometry yielded a structure with C_2 symmetry (figure 1), the average Si–C bond distance of 1.822 Å. The energy cost to replace one C atom with Si, calculated by taking the total energy difference, namely $\Delta E = E(C_{59}Si) + E(C) - E(C_{60}) - E(Si)$, is 5.080 eV. These are in agreement with previous calculations and experiments [34–37].

For $C_{59}Si$ the energy gap between the highest occupied molecular orbital (HOMO) and the lowest unoccupied molecular orbital (LUMO) is 1.17 eV, lower than that (1.61 eV) of C_{60}. Furthermore, the HOMO and LUMO were mainly concentrated on the Si site and its neighboring C sites. Because of the difference in electronegativity between C and Si, charge is transferred from Si to C allowing $C_{59}Si$ to have a dipole moment of 1.42 D. From the geometry, charge distribution and frontier orbitals, we can clearly see the anisotropy induced by Si doping. Thus, the Si site can thus be used as a 'seed' for anisotropic growth when ligand molecules are attached. This is demonstrated in the following by using Si_{10}, $Si_{12}W$, $Si_{16}Ti$ and $Si_{20}Ba$ as ligands.

3.1. Si_{10} interacting with $C_{59}Si$

Silicon clusters in the size ranges of 3–12 were initially synthesized in a supersonic beam in 1987 [38]. The ultraviolet photoelectron spectra (UPS) data suggested that among these clusters, those containing 4, 6, 7 and 10 Si atoms are magic. Since then, many experimental and theoretical studies have concentrated on the Si_{10} cluster [39–41] which has a tetracapped trigonal prism structure with C_{3v} symmetry. The relaxed structure is plotted in figure 2, together with its HOMO and LUMO images. We see that the HOMO is mainly concentrated on the bottom triangular face, while the LUMO originates from both the bottom and the top triangular face. The HOMO–LUMO gap is 2.09 eV.

Based on the distribution of orbitals in $C_{59}Si$, we can expect that the Si site should be the most likely absorption site [42]. For Si_{10} we consider two possible configurations interacting with $C_{59}Si$: configuration I where Si_{10} binds to the Si atom in $C_{59}Si$ through its bottom triangular face or configuration II where Si_{10} binds through its top triangular face. For configuration I, the optimized geometry and electronic structure are shown in figure 3. The interaction

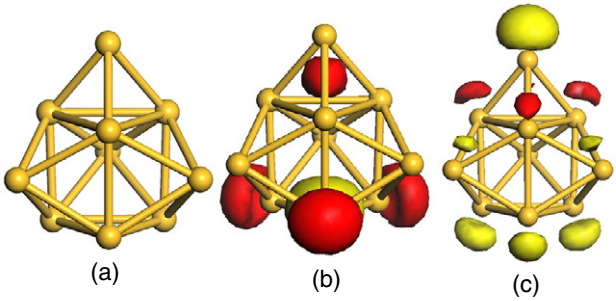

Figure 2. Geometry (a), HOMO (b) and LUMO (c) of the Si_{10} cluster.

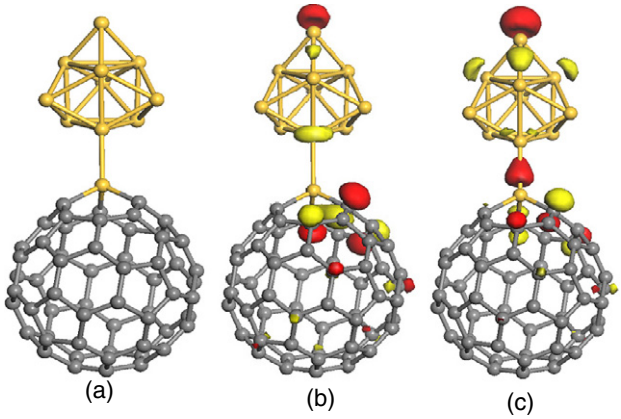

Figure 3. (a) Geometry, (b) HOMO and (c) LUMO of the $C_{59}Si$–Si_{10} cluster.

energy, defined as, $\Delta E = -[E(C_{59}Si\text{–}Si_{10}) - E(C_{59}Si) - E(Si_{10})]$, is calculated to be 1.15 eV with the linking Si–Si distance of 2.441 Å and the HOMO–LUMO gap of 0.65 eV. For configuration II, the adsorption energy is 0.86 eV, weaker than that in configuration I, while the bond length of the Si–Si is enlarged to 2.475 Å. In figure 3, we also see that both the HOMO and LUMO orbitals of the $C_{59}Si$–Si_{10} complex are mainly concentrated on the Si part and the atoms near the Si site. Therefore the introduction of Si_{10} into $C_{59}Si$ has enhanced the anisotropy of the structure. Furthermore, because of the difference in electronegativity between C and Si, charge is likely to transfer from Si to C. In fact Si in $C_{59}Si$ carries a charge of +0.852, which is increased to +0.996 when interacting with Si_{10}. The charges are redistributed in the system, in particular the linking Si site in the Si_{10} unit carries a charge of −0.236, and the three C atoms linking with Si in $C_{59}Si$ become more negatively charged, as shown in figure 4. The charge redistribution in $C_{59}Si$–Si_{10} results in a large dipole moment of 7.11 D. The frontier orbital distributions clearly indicate that the Si sites and their neighboring C sites are much more active than other sites.

3.2. *W@Si_{12} interacting with $C_{59}Si$*

W@Si_n clusters were synthesized using an ion trap by reacting the transition metal ion, W^+ with silane (SiH_4). The W@Si_{12} cluster was found experimentally to be magic and stable, which

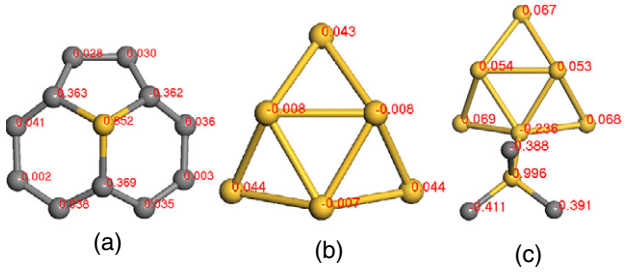

Figure 4. Charge distribution of (a) $C_{59}Si$, (b) Si_{10} and (c) $C_{59}Si$–Si_{10}.

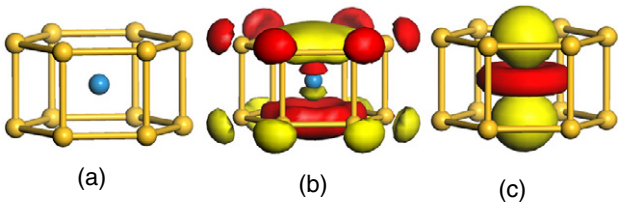

Figure 5. (a) Geometry, (b) HOMO and (c) LUMO of W@Si_{12} cluster.

was also confirmed by *ab initio* calculation. In W@Si_{12}, the W atom is encapsulated inside a Si_{12} cage, having a hexagonal-shaped cage with D_{6h} symmetry. The stability of this structure is due to both the electronic and the geometrical shell closures [8, 43].

We began the calculations by optimization on the W@Si_{12} cage, plotted in figure 5 (the bonds connecting the Si atom with W in the center are omitted for clarity). The relaxed structure is a hexagonal cage as expected. There are two types of Si–Si bond lengths: 2.381 Å on the top and bottom faces and 2.402 Å in the lateral edges. The bond length between Si and W is 2.667 Å. Its HOMO–LUMO gap W@Si_{12} is calculated to be 1.37 eV. These data agree well with the results in [41]. Note that the HOMO of W@Si_{12} mainly reside on two hexagon rings, and the LUMO arises mainly from d_{z2}-W.

To optimize the geometry of $Si_{12}W$ interacting with $C_{59}Si$, we began with an initial geometry where the Si site in $C_{59}Si$ is connected to the hexagonal ring of $Si_{12}W$. The optimized structure is shown in figure 6, together with the HOMO and LUMO plots. We find that the W@Si_{12} is slightly distorted, and tilted at an angle of 55° with respect to the initial orientation to make the two linking Si atoms four-fold coordinated as required by sp^3 hybridization. The bond length between the two linking Si atoms is 2.434 Å. The corresponding adsorption energy is 1.06 eV and the HOMO–LUMO gap is reduced to 0.43 eV. This is much lower than those of the individual units (1.17 eV for $C_{59}Si$, and 1.37 eV for W@Si_{12}). Unlike $C_{59}Si$–Si_{10}, there is only a small amount of charge transfer between these two units (see figure 7). However, the frontier orbitals clearly show the anisotropy of the $C_{59}Si$–$Si_{12}W$ complex, where the Si and the neighboring C sites are much more reactive. What is more important is that this complex has a large dipole moment of 8.04 D. This character may be very useful for materials self-assembly under an applied electric field.

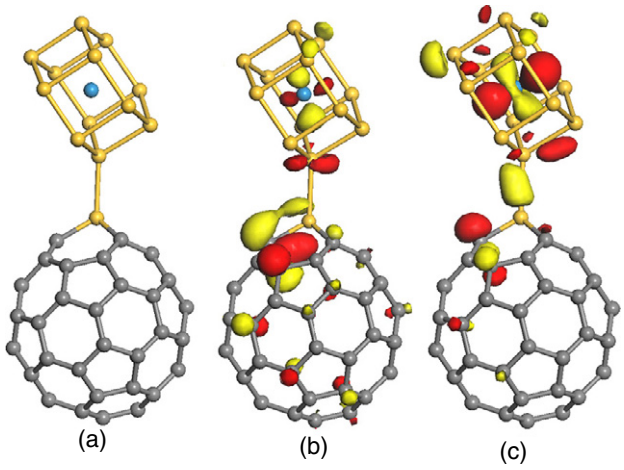

Figure 6. (a) Geometry, (b) HOMO and (c) LUMO of $C_{59}Si$–$W@Si_{12}$ cluster.

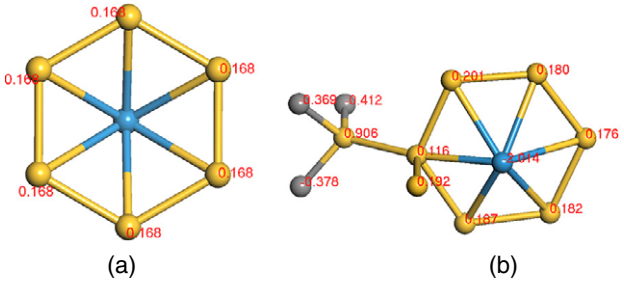

Figure 7. Charge distributions in (a) $W@Si_{12}$ and (b) $C_{59}Si$–$W@Si_{12}$ (partial atoms in the cluster).

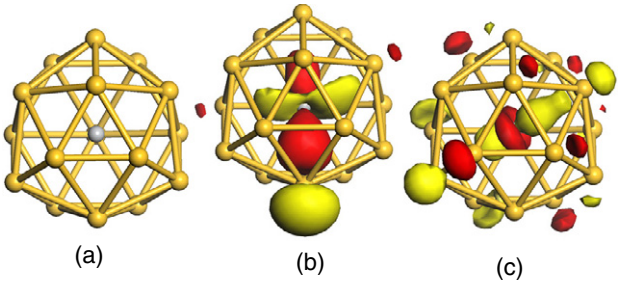

Figure 8. (a) Geometry, (b) HOMO and (c) LUMO of $Ti@Si_{16}$ cluster.

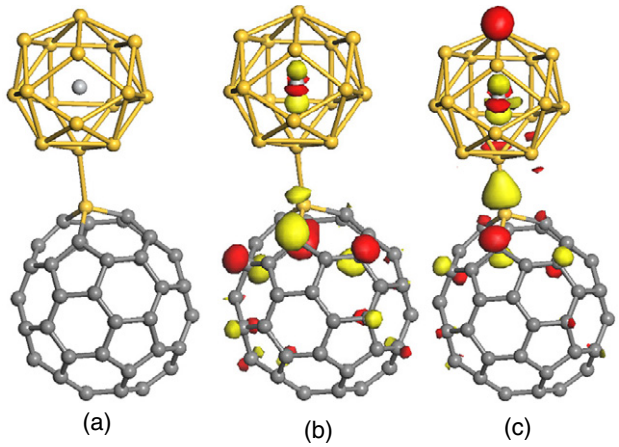

Figure 9. (a) Geometry, (b) HOMO and (c) LUMO of $C_{59}Si$-$Ti@Si_{16}$ cluster.

3.3. $Ti@Si_{16}$ interacting with $C_{59}Si$

The $Ti@Si_{16}$ cage has been synthesized by a combination of a laser vaporization method and a flow-tube reactor [44]. Extensive investigations [45, 46] have confirmed that this cluster possesses a truncated tetrahedral structure, called the Frank–Kasper (FK) polyhedron, with T_d symmetry. The optimized structure is shown in figure 8 along with its HOMO and LUMO orbitals. Among the 28 triangles, there are four truncated triangles with bond lengths of 2.437 Å, with the remaining 24 being of one type with bond lengths of about 2.658 Å. We point out that an isolated Ti atom has an electronic configuration of $3d^2 4s^2$ and a magnetic moment of 2 μ_B, which is quenched when encapsulated in Si_{16} cage. Is it possible to recover this magnetic moment when this cluster is attached to $C_{59}Si$? Actually if the attachment can expand the Si cage, the increased Si–W bond length will lead to less orbital hybridization between W and its neighboring Si atoms. Hence, the magnetic moment of Ti can be retained.

Motivated by this expectation, we studied the interaction between $C_{59}Si$ and $Si_{16}Ti$. As discussed above, $Si_{16}Ti$ has two inequivalent types of triangles which were respectively attached to the Si site in $C_{59}Si$ in optimizing the geometry. The preferred structure is shown in figure 9. The two cages are connected with each other through a single Si–Si bond (2.496 Å). The corresponding binding energy and HOMO–LUMO gaps are respectively 0.93 eV, and 0.56 eV. The Si site in $C_{59}Si$ interacts with the Si in $Ti@Si_{16}$ along the on-top direction. Because of this interaction, the structure of the $Ti@Si_{16}$ cage is distorted and the symmetry is changed to C_{3v}. The cage is only slightly expanded, but not enough to significantly reduce orbital hybridization. Hence, the $Ti@Si_{16}$ complex maintains its non-magnetic character, but displays a huge dipole moment of 9.18 D. The attachment also changes the orbital distributions. In contrast to figure 8(c) where the LUMO of $Si_{12}W$ mainly derives from Si sites on the cage surface and W site in the center, in the $Ti@Si_{16}$ complex the contribution from the Si cage surface is reduced (see figure 9(c)). The top part of Si cage and the Si site in $C_{59}Si$ together with its neighboring C sites become reactive.

3.4. $Ba@Si_{20}$ interacting with $C_{59}Si$

The structure of Si_{20} is of special interest since the smallest fullerene cage is C_{20}. However, Si_{20} consists of two Si_{10} forming a compact structure. The cage structure can be stabilized by encapsulating one Ba atom [5], as shown in figure 10(a). The bond length of Si–Si is 2.357 Å and the distance of the center Ba atom to Si is 3.301 Å. The HOMO–LUMO gap of the cage is 0.58 eV. Different from the case of $Si_{16}Ti$, the HOMO and LUMO arise mainly from Si atoms but not from the metal atom (see figures 10(b) and (c)). Due to the cage's highest symmetry, every atom is equivalent. Thus, to optimize the geometry we initially put the pentagonal

Table 1. Bond lengths between linking Si atoms, binding energy, HOMO–LUMO gap, and dipole moment of the various complexes studied.

Cluster	Linking bond length (Å)	Binding energy (eV)	HOMO–LUMO gap (eV)	Dipole moment (D)
$C_{59}Si$–Si_{10}	2.441	1.15	0.65	7.11
$C_{59}Si$–$W@Si_{12}$	2.434	1.06	0.44	8.04
$C_{59}Si$–$Ti@Si_{16}$	2.496	0.93	0.56	9.18
$C_{59}Si$–$Ba@Si_{20}$	2.354	1.89	0.58	3.96

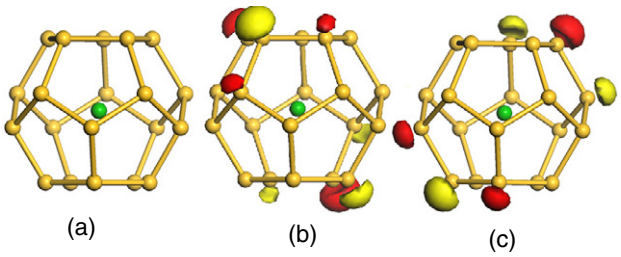

Figure 10. (a) Geometry, (b) HOMO and (c) LUMO of the $Ba@Si_{20}$ cluster.

face of the $Ba@Si_{20}$ above the Si top site in $C_{59}Si$. After optimization, the $Ba@Si_{20}$ cage prefers to connect with the $C_{59}Si$ heterofullerene through a single Si–Si bond with a bond length of 2.354 Å and a tilt angle of about 30° with respect to the initial orientation, see figure 11. The absorption energy of this system is 1.88 eV, which is larger than the others. The reason is the following: in $Ba@Si_{20}$ the Si sites are negatively charged due to the charge transfer from Ba [5], while the Si site in $C_{59}Si$ is positively charged, which results in a large binding energy and a small linking distance when these two units bind together. Its HOMO–LUMO gap is 0.58 eV, and the dipole moment is found to be 3.96 D. It is interesting to note that the interactions between these two units change the orbital distributions. For example, the HOMO in the complex structure is mainly concentrated on the $Ba@Si_{20}$ cage, while the LUMO is predominantly on C sites nearest to the Si site in $C_{59}Si$. This suggests that if the LUMO of some species is close to the HOMO of $C_{59}Si$–$Si_{20}Ba$ in energy, then these species would preferably attach to the Si cage. On the other hand, if the HOMO of some species is close to the LUMO of $C_{59}Si$–$Si_{20}Ba$ in energy, then these species will preferably attach to the C cage. Therefore, selective functionalization can be realized in this system.

4. Conclusions

The similarities and differences between Si and C, as well as their potential applications, make studies of the Si–C Janus structures very attractive. In this paper, we have systematically studied the interactions between Si-doped fullerene $C_{59}Si$ and experimentally synthesized and well studied Si clusters including Si_{10}, $Si_{12}W$, $Si_{16}Ti$, and $Si_{20}Ba$. In table 1 we have summarized the main results of our work and arrived at the following conclusions:

(1) The Si atom in the heterofullerene provided the attachment site for the ligands during the anisotropic growth of Janus nanostructures.

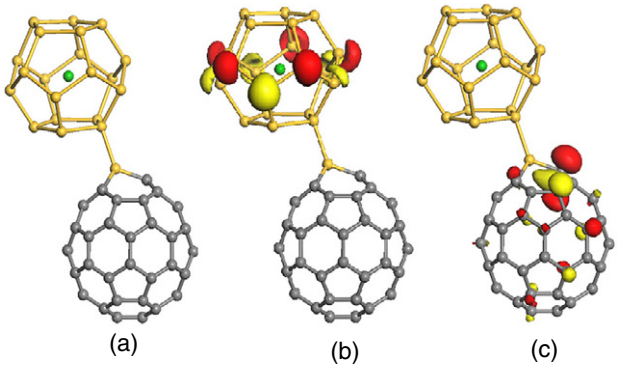

Figure 11. (a) Geometry, (b) HOMO and (c) LUMO of $C_{59}Si$–$Ba@Si_{20}$ cluster.

(2) The Si site in $C_{59}Si$ is more reactive than the C atoms.
(3) When a Si cluster is attached to $C_{59}Si$, it preferentially interacts with the Si atom of the ligand cluster along the on-top direction.
(4) Si–C Janus nanostructures thus formed exhibit enhanced anisotropic properties. They display large dipole moments and hence can form self-assembled materials under the influence of an external electric field.
(5) The attachment of Si clusters to $C_{59}Si$ provides a simple pathway to fabricate silicon–carbon Janus anisotropic nanostructures.

Acknowledgments

This work is partially supported by grants from the National Natural Science Foundation of China (NSFC-10744006, NSFC-10874007) and from the US Department of Energy.

References

[1] de Gennes P G 1992 *Rev. Mod. Phys.* **64** 645
[2] Kroto H W, Heath J R, O'Brien S C, Curl R F and Smalley R E 1985 *Nature* **318** 162
[3] Krätshmer W, Lamb L D, Fostiropoulos K and Huffman D R 1990 *Nature* **347** 354
[4] Hiura H, Miyazaki T and Kanayama T 2001 *Phys. Rev. Lett.* **86** 1733
[5] Kumar V and Kawazoe Y 2001 *Phys. Rev. Lett.* **87** 045503
[6] Sun Q, Wang Q, Briere T M, Kumar V, Kawazoe Y and Jena P 2002 *Phys. Rev.* B **65** 235417
[7] Sun Q, Wang Q, Jena P, Rao B K and Kawazoe Y 2003 *Phys. Rev. Lett.* **90** 135503
[8] Sun Q, Wang Q, Briere T M and Kawazoe Y 2002 *J. Phys.: Condens. Matter* **14** 4503
[9] Melinon P, Masenelli B, Tournus F and Perez A 2007 *Nat. Mater.* **6** 79

[10] Sun Q, Wang Q, Kawazoe Y and Jena P 2002 *Phys. Rev.* B **66** 245425
[11] Harada M, Osawa S, Osawa E and Jemmis E D 1994 *Chem. Lett.* **1** 1037
[12] Osawa S, Harada M and Osawa E 1995 *Fullerene Sci. Technol.* **3** 225
[13] Jemmis D E, Leszczynski J and Osawa E 1998 *Fullerene Sci. Technol.* **6** 271
[14] Sheka E F, Nikitina E A, Zayets V A and Ginzburg I Y 2002 *Int. J. Quantum Chem.* **88** 441
[15] Tanaka H, Osawa S, Onoe J and Takeuchiet K 1999 *J. Phys. Chem.* B **103** 5939
[16] Gong X G and Zheng Q Q 1995 *Phys. Rev.* B **52** 4756
[17] Kimura T, Sugai T and Shinohara H 1996 *Chem. Phys. Lett.* **256** 269
[18] Pellarin M, Ray C, Mélinon P, Lermé J, Vialle J L, Kéghélian P, Perez A and Broyer M 1997 *Chem. Phys. Lett.* **277** 96
[19] Ray C, Pellarin M, Lermé J L, Vialle J L, Broyer M, Blase X, Mélinon P, Kéghélian P and Perez A 1998 *Phys. Rev. Lett.* **80** 5365
[20] Pellarin M, Ray C, Lermé J, Vialle J L, Broyer M, Blase X, Mélinon P, Kéghélian P and Perez A 1999 *J. Chem. Phys.* **110** 6927
[21] Pellarin M, Ray C, Lermé J, Vialle J L, Broyer M, Blase X, Kéghélian P, Mélinon P and Perez A 1999 *Eur. Phys. J.* D **9** 49
[22] Pellarin M, Ray C, Lermé J, Vialle J L, Broyer M and Mélinon P 2000 *J. Chem. Phys.* **112** 8436
[23] Ohara M, Nakamura Y, Negishi Y, Miyajima K, Nakajima A and Kaya K 2002 *J. Phys. Chem.* A **106** 4498
[24] Tournus F, Masenelli B, Mélinon P, Blase X, Perez A, Pellarin M, Broyer M, Flank A M and Lagarde P 2002 *Phys. Rev.* B **65** 165417
[25] Klajn R, Bishop K J M, Fialkowski M, Paszewski M, Campbell C J, Gray T P and Grzybowski B A 2007 *Science* **316** 261
[26] Glotzer S C and Solomon M J 2007 *Nat. Mater.* **6** 557
[27] Shevchenko E V, Talapin D V, Kotov N A, O'Brien S and Murray C B 2006 *Nature* **439** 55
[28] Blaaderen A V 2006 *Nature* **439** 545
[29] Leunissen M E 2005 *Nature* **437** 325
[30] Roh K-H, Martin D C and Lahann J 2005 *Nat. Mater.* **4** 759
[31] Wang Y and Perdew J P 1991 *Phys. Rev.* B **44** 13298
[32] Blochl P 1994 *Phys. Rev.* B **50** 17953
[33] Kresse G and Joubert J 1999 *Phys. Rev.* B **59** 1758
[34] Lu J, Luo Y, Huang Y, Zhang X and Zhao X 2001 *Solid State Commun.* **118** 309
[35] Tomekia M S, Ilya Y and Jerzy L 2005 *Int. J. Quantum Chem.* **105** 429
[36] Billas I M L, Massobri C, Boero M, Parrinello M, Branze W, Malinowski N, Heinebrodt M and Martin T P 1999 *J. Chem. Phys.* **111** 67
[37] Ray C, Pellarin M, Lermé J L, Viallel J L, Broyer M, Blase X, Melinon P, Keghelian P and Perez A 1998 *Phys. Rev. Lett.* **80** 53
[38] Cheshnovsky O, Yang S H, Pettiette C L, Craycraft M J, Liu Y and Smalley R E 1987 *Chem. Phys. Lett.* **138** 119
[39] Nigam S, Majumder C and Kulshreshtha S K 2004 *J. Chem. Phys.* **121** 16
[40] Yang J C, Xu W G and Xiao W S 2005 *J. Mol. Struct. THEOCHEM* **98** 719
[41] Nigam S, Majumder C and Kulshreshtha S K 2006 *J. Chem. Phys.* **125** 074303
[42] Wu M M, Sun Q, Wang Q, Jena P and Kawazoe Y 2009 *J. Chem. Phys.* **130** 184714
[43] Lu J and Nagase S 2003 *Phys. Rev. Lett.* **90** 115506
[44] Ohara M, Koyasu K, Nakajima A and Kaya K 2003 *Chem. Phys. Lett.* **371** 490
[45] Kumar V, Briere T M and Kawazoe Y 2003 *Phys. Rev.* B **68** 155412
[46] Kawamura H, Kumar V and Kawazoe Y 2005 *Phys. Rev.* B **71** 075423